

Table VIII. Probable Hydrogen Bonds in $(\text{CN}_3\text{H}_6)_2[(\text{CH}_3)_2\text{AsMo}_4\text{O}_{15}\text{H}]\cdot\text{H}_2\text{O}$

atoms	symmetry operation	dist, Å
H(2)-O(1)	$1-x, -y, 1-z$	2.081 (6) ^a
H(3)-O(15)	$x-1, y, z$	1.908 (6)
H(10)-O(12)	x, y, z	2.218 (6)
H(11)-O(13)	$-x, y-1/2, 1/2-z$	1.985 (5)
H(12)-O(15)	$-x, y-1/2, 1/2-z$	2.072 (6)
H(13)-O(10)	$1-x, y-1/2, 1/2-z$	2.129 (7)
H(14)-O(9)	x, y, z	1.838 (5)
H(15)-O(8)	$1-x, 1/2+y, 1/2-z$	2.007 (6)
H(16)-O(3)	x, y, z	2.103 (6)
H(17)-O(7)	$1-x, -y, 1-z$	2.024 (7)
H(19)-O(16)	$x, -y-1/2, z-1/2$	1.951 (6)
H(20)-O(4)	x, y, z	2.176 (8)
H(21)-O(5)	$1-x, -y, 1-z$	2.174 (6)

^a The standard error in parentheses after each parameter refers to the last decimal place given.

offer advantages and both have their limitations. In polyanion structures, where the locations of the protons are known, the latter are found to be attached to those sterically accessible oxygen atoms that bridge the most metal atoms. This is not surprising since M-O bond lengths to such oxygens are likely to be long and will result in low total bond orders at the oxygen and therefore a relatively high negative charge. Klemperer and Shum have verified this principle in their ¹⁷O NMR study³⁴ of the protonation of $\text{V}_{10}\text{O}_{28}^{6-}$. In the tetramolybdosarsinate structure, the proton is attached to the unusual

four-coordinate oxygen. The Mo-O bond lengths to this oxygen atom are very long and imply a low (<0.2³⁵) bond order. The asymmetric position of the oxygen in the Mo_4 frame is considered to result from the presence of the hydrogen-bonded water molecule which lies toward the longest Mo-O(H) bond. In the structure of $(\text{Bu}_4\text{N})_3\text{CH}_2\text{Mo}_4\text{O}_{15}\text{H}$, which has no such water molecule, the corresponding oxygen atom is more nearly equidistant from the four molybdenum atoms.

Acknowledgment. This work has been supported in part by the Office of Naval Research. The neutron diffraction measurements were made while K.M.B. was a guest worker at the National Bureau of Standards.

Registry No. $(\text{CN}_3\text{H}_6)_2[(\text{CH}_3)_2\text{AsMo}_4\text{O}_{15}\text{H}]\cdot\text{H}_2\text{O}$, 56652-65-4; $\text{Na}_2[(\text{CH}_3)_2\text{AsMo}_4\text{O}_{15}\text{H}]$, 73804-99-6; $[(\text{CH}_3)_4\text{N}]_2[(\text{CH}_3)_2\text{AsMo}_4\text{O}_{15}\text{H}]$, 73805-00-2; $\text{K}_2[(\text{CH}_3)_2\text{AsMo}_4\text{O}_{15}\text{H}]$, 73816-05-4; $[(\text{C}_4\text{H}_9)_4\text{N}]_2[(\text{CH}_3)_2\text{AsMo}_4\text{O}_{15}\text{H}]$, 68109-04-6; $[(\text{C}_4\text{H}_9)_4\text{N}]_2[(\text{CH}_3)_2\text{AsMo}_4\text{O}_{15}\text{D}]$, 73805-02-4; $(\text{CN}_3\text{H}_6)_2[(\text{C}_2\text{H}_5)_2\text{AsMo}_4\text{O}_{15}\text{H}]$, 73805-04-6; $\text{K}_2[(\text{C}_2\text{H}_5)_2\text{AsMo}_4\text{O}_{15}\text{H}]$, 73805-05-7; $\text{Na}_2[(\text{C}_2\text{H}_5)_2\text{AsMo}_4\text{O}_{15}\text{H}]$, 73805-06-8; $[(\text{CH}_3)_4\text{N}]_2[(\text{C}_2\text{H}_5)_2\text{AsMo}_4\text{O}_{15}\text{H}]$, 73805-07-9; $[(\text{C}_4\text{H}_9)_4\text{N}]_2[(\text{C}_2\text{H}_5)_2\text{AsMo}_4\text{O}_{15}\text{H}]$, 73805-08-0; $\text{Na}_2[(\text{C}_6\text{H}_5)_2\text{AsMo}_4\text{O}_{15}\text{H}]$, 73816-06-5; $\text{K}_2[(\text{C}_6\text{H}_5)_2\text{AsMo}_4\text{O}_{15}\text{H}]$, 73816-07-6; $(\text{CN}_3\text{H}_6)_2[(\text{C}_6\text{H}_5)_2\text{AsMo}_4\text{O}_{15}\text{H}]$, 73816-09-8; $[(\text{CH}_3)_4\text{N}]_2[(\text{C}_6\text{H}_5)_2\text{AsMo}_4\text{O}_{15}\text{H}]$, 73825-15-7; $[(\text{C}_4\text{H}_9)_4\text{N}]_2[(\text{C}_6\text{H}_5)_2\text{AsMo}_4\text{O}_{15}\text{H}]$, 68081-63-0; $[(\text{C}_6\text{H}_5)_4\text{As}]_2[(\text{C}_6\text{H}_5)_2\text{AsMo}_4\text{O}_{15}\text{H}]$, 73816-10-1; sodium molybdate, 7631-95-0.

Supplementary Material Available: Tables of final calculated and observed structure factors (47 pages). Ordering information is given on any current masthead page.

(34) Klemperer, W. G.; Shum, W. J. *Am. Chem. Soc.* 1977, 99, 3544.

(35) Schroeder, F. A. *Acta Crystallogr., Sect. B* 1975, B31, 2294.

Contribution from the Istituto di Chimica delle Macromolecole del CNR, 20133 Milano, Italy

Meshing Ability of Bulky Tertiary Phosphines. X-ray Structure of *cis*-Bis(di-*tert*-butylphenylphosphine)dichloroplatinum(II)

W. PORZIO, A. MUSCO, and A. IMMIRZI*

Received December 28, 1979

The square-planar platinum(II) complex $\text{PtCl}_2(\text{P}(t\text{-Bu})_2\text{Ph})_2$, containing two bulky phosphines *cis* to each other, has been studied by X-ray diffraction methods. The crystals are monoclinic of space group $P2_1/c$, with $a = 11.211$ (1) Å, $b = 14.621$ (1) Å, $c = 18.157$ (2) Å, $\beta = 102.38$ (2)°, and $Z = 4$. The structure was solved by Patterson and Fourier methods and refined by least squares to a conventional R factor of 0.059, on the basis of 2427 intensities above background. The square-planar coordination is very distorted with P-Pt-P and Cl-Pt-Cl angles of 107.3 (4) and 84.2 (3)°, respectively. The mean Pt-P and Pt-Cl distances are 2.358 (6) and 2.333 (5) Å. The stability of the complex, in spite of the *cis* relation of the two phosphines, is explained as having recourse to the variable-aperture cone model. The substituent orientation about the Pt-P bonds allows for a good fitting of protrusions and hollows without severe steric hindrance.

Introduction

Electronic properties and size of the ligands play an important role in the reactions catalyzed by transition-metal phosphine complexes.¹ The cone angle introduced by Tolman is a simple criterion to measure the ligand size. The steric demand of the ligand may also be measured in terms of solid cone angles.²

Di-*tert*-butylphenylphosphine $\text{P}(t\text{-Bu})_2\text{Ph}$ is a very bulky ligand which has a ligand cone angle $\theta = 170^\circ$ and a solid cone angle $\Omega = 4.55$ rad, respectively. With this phosphine the only

zerovalent PtL_n stable complex is PtL_2 , and no appreciable quantity of PtL_3 is formed in solution even in the presence of a large excess of free phosphine.³ For these reasons one expects that only the *trans* isomer will be stable in the square-planar complex PtCl_2L_2 . Recently an orange crystalline product which analyzes as $\text{PtCl}_2(\text{P}(t\text{-Bu})_2\text{Ph})_2$ has been isolated in our laboratory. As the color is different from the yellow *trans*- $\text{PtCl}_2(\text{P}(t\text{-Bu})_2\text{Ph})_2$ described by Shaw,⁴ the crystals were studied by X-ray diffraction methods. The compound proved to be the unexpected *cis*- $\text{PtCl}_2(\text{P}(t\text{-Bu})_2\text{Ph})_2$.

(1) Tolman, C. A. *Chem. Rev.* 1977, 77, 313.

(2) Immirzi, A.; Musco, A. *Inorg. Chim. Acta* 1977, 25, L41.

(3) Mann, B. E.; Musco, A. *J. Chem. Soc., Dalton Trans.*, in press.

(4) Mann, B. E.; Shaw, B. L.; Slade, R. M. *J. Chem. Soc. A* 1971, 2976.

Table I. Crystal Data and Working Conditions of the Molecule

$\text{PtCl}_2\text{P}_2\text{C}_{28}\text{H}_{46}$	$M_r = 710.63$
$a = 11.211 (1) \text{ \AA}$	$d_{\text{calcd}} = 1.65 \text{ g}\cdot\text{cm}^{-3}$
$b = 14.621 (1) \text{ \AA}$	space group $P2_1/c$ (No. 14)
$c = 18.157 (2) \text{ \AA}$	$\mu_{\text{MoK}\alpha} = 52.7 \text{ cm}^{-1}$
$\beta = 102.38 (2)^\circ$	$F(000) = 1424 \text{ e/cell}$
$V = 2861.0 (1) \text{ \AA}^3$	
scan method: ω	
scan speed: $2.4^\circ/\text{min}$	
scan width: 1.2°	
bkgd time: $2 \times 10 \text{ s}$	
θ range (d_{min}): $3\text{--}24^\circ (0.87 \text{ \AA})$	
measd reflctns: 4545	
"obsd" reflctns ($I > 3\sigma$, $\sigma^2 = \text{peak} - \text{counts} +$	
total bkgd counts): 2427	
wavelength: 0.71069 \AA	
approx cryst size: $0.1 \times 0.08 \times 0.08 \text{ mm}^3$	

The stability of this compound makes a detailed structural analysis, with particular reference to the ligand conformations, very desirable.

Experimental Section

Crystals of *cis*- $\text{PtCl}_2(\text{P}(t\text{-Bu})_2\text{Ph})_2$ suitable for X-ray studies were obtained by slow addition of diethyl ether acidified with aqueous hydrochloric acid to an ethereal solution of $\text{Pt}(\text{P}(t\text{-Bu})_2\text{Ph})_2\text{O}_2$.⁵ The measurements were performed by means of a Philips PW 1100 single-crystal diffractometer in the conditions given in Table I. Accurate lattice constants were obtained through a least-squares optimization using the θ values of 30 strong reflections ($6^\circ < \theta < 24^\circ$) evaluated as centers of gravity of the profiles $I = f(\theta)$ and averaging over positive and negative θ values.

Structure Determination. The atomic positions of the nonhydrogen atoms for $\text{PtCl}_2(\text{P}(t\text{-Bu})_2\text{Ph})_2$ were determined by the heavy-atom method and refined by the least-squares method minimizing $\sum w(F_o - F_c)^2$ with unitary weight factors in the block-diagonal approximation.⁶ The atomic scattering factors (neutral atoms) and the correction $\Delta f'$ and $\Delta f''$ for the anomalous dispersion for Pt, Cl, and P were taken from ref 7. The conventional *R* factor was reduced to 0.069 by using anisotropic thermal parameters for the Pt, Cl, and P atoms only and to 0.061 by allowing anisotropic vibrations for the carbon atoms also. At this stage the difference electron density map revealed some residual peaks with weights from 3.0 to 0.5 e \AA^{-3} , mainly due to series truncation effects. Other scattered peaks were in inconsistent positions to be assigned to the hydrogen atoms. However hydrogen atoms were included in calculated positions on assumption of ideal sp^2 and sp^3 local geometries about the carbon atoms and staggered conformations of the methyl groups with respect to phosphorus atoms; isotropic thermal vibration parameters for H atoms were assumed to be 1.2 times the isotropic value of the parent carbon atom. After inclusion of H atom contributions and a few refinement cycles, *R* was reduced to 0.059.

The final fractional coordinates and anisotropic thermal vibration parameters are listed in Table II.

Coordination Geometry. The crystal structure consists of the packing of discrete molecules of $\text{PtCl}_2(\text{P}(t\text{-Bu})_2\text{Ph})_2$. In Table III the relevant interatomic distances, bond angles, and torsion angles are reported; the equations of some relevant molecular planes are given in Table IV and the shortest packing distances are reported in Table V.

As shown in Figure 1 the *cis* square-planar structure is very distorted; the distortion is visible both from the bond angles at Pt (see Table III) and from the dihedral angle between Cl–Pt–Cl and P–Pt–P planes (31.5°).

Similar distortions in Pt(II) and Pd(II) square-planar complexes have been already observed in few cases. For instance in $\text{PtCl}[\text{PPh}(t\text{-Bu})(i\text{-Pr})](\text{C}_{14}\text{H}_{16}\text{N})$ ⁸ the four substituents are displaced from the averaged coordination plane by 0.03, -0.12 , 0.48 , and -0.38 \AA ,

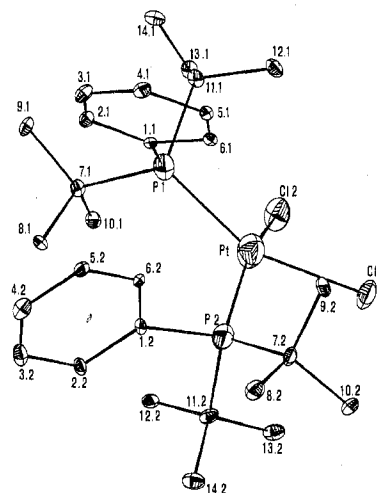


Figure 1. The ORTEP drawing of the molecule, viewed along the *c* axis. For the sake of clarity the carbon atoms are labeled with numbers only.

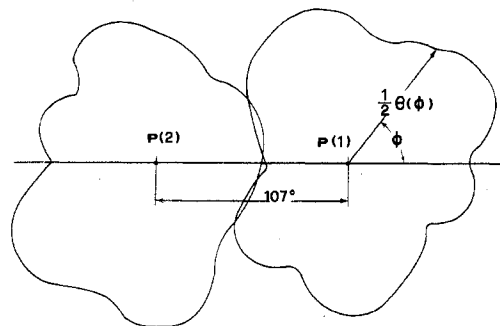


Figure 2. The two irregular curves are polar representations of the variable-aperture cones (defined according ref 2) corresponding to the two $\text{P}(t\text{-Bu})_2\text{Ph}$ phosphines, of different shape, observed in the *cis*- $\text{PtCl}_2(\text{P}(t\text{-Bu})_2\text{Ph})_2$ complex. The angular coordinate ϕ is the rotation about the Pt–P bond, and the radial coordinate is proportional to the corresponding cone aperture $1/2\theta$. The two cones are oriented like the phosphines in the complex and their centers are separated by 107.3° , i.e., the observed P–Pt–P angle.

in *cis*- $\text{Pt}(\text{PPh}_3)_2[\text{P}(\text{C}_6\text{F}_5)_2]_2$ ⁹ by 0.15, -0.16 , 0.28 , and -0.28 \AA , and in $\text{Pt}(\text{PPh}_3)_2\text{Cl}(\text{C}_3\text{H}_7)$ ¹⁰ by -0.06 , -0.02 , 0.14 , and -0.29 \AA . In ref 9 the value of 20.4° is reported for the above defined dihedral angle.

The geometry of the PtCl_2P_2 frame may be compared with that of *cis*- PtCl_2DTE ¹¹ and *cis*- PtCl_2DTP ¹² (DTE = 1,2-bis(di-*tert*-butylphosphino)ethane; DTP = 1,3-bis(di-*tert*-butylphosphino)propane), both bidentate ligands, which have angles between the Cl–Pt–Cl and P–Pt–P planes of 0.0 and 12.0° , respectively.

The mean Pt–P distance $2.332 (5) \text{ \AA}$ is larger than that occurring in the DTP case ($2.282 (3) \text{ \AA}$) and still larger than that in the DTE case ($2.264 (3) \text{ \AA}$). The increasing bond length seems to correspond to the increasing distortion. The mean Pt–Cl distances are comparable in the three cases, while the Cl–Pt–Cl angles $84.2 (3)^\circ$ in our case, $86.3 (1)^\circ$ for DTE, and $83.2 (1)^\circ$ for DTP are slightly different and do not correlate with the increasing distortion.

The crystal packing was analyzed (see Table V) by using calculated positions for the aromatic H atoms and assuming spherical CH_3 groups. Only the three distances marked with asterisks appear somewhat shorter than the standard van der Waals contacts. This fact should not imply an appreciable influence of the packing on the molecular shape.

(5) Yoshida, T.; Otsuka, S. *J. Am. Chem. Soc.* **1977**, *99*, 2134.

(6) All the computer programs used here were written by A. Immirzi (version for Univac 1100 computer).

(7) "International Tables for X-ray Crystallography"; Kynoch Press: Birmingham, England, 1974; Vol. IV, pp 99, 149.

(8) Tani, K.; Brown, L. D.; Ahmed, J.; Ibers, J. A.; Yokota, M.; Nakamura, A.; Otsuka, S. *J. Am. Chem. Soc.* **1977**, *99*, 7876.

(9) Elmes, P. S.; Scudder, M. L.; West, B. O. *J. Organomet. Chem.* **1976**, *122*, 281.

(10) Furlani, A.; Russo, M. V.; Villa, A. C.; Manfredotti, A. G.; Guastini, C. *J. Chem. Soc., Dalton Trans.* **1977**, 2154.

(11) Harada, M.; Kai, Y.; Yasuoka, N.; Kasai, N. *Bull. Chem. Soc. Jpn.* **1976**, *49*, 3472.

(12) Harada, M.; Kay, Y.; Yasuoka, N.; Kasay, N., *Bull. Chem. Soc. Jpn.* **1979**, *52*, 390.

Table II. Atomic Fractional Coordinates ($\times 10^3$ for Pt and $\times 10^4$ for the Other Atoms) and Anisotropic Thermal Vibration Parameters ($\times 10^2$ for Pt and $\times 10$ for the Other Atoms) of the Molecule, with Esd's in Parentheses^a

atom	<i>x/a</i>	<i>y/b</i>	<i>z/c</i>	<i>U</i> ₁₁	<i>U</i> ₂₂	<i>U</i> ₃₃	<i>U</i> ₁₂	<i>U</i> ₁₃	<i>U</i> ₂₃
Pt	22714 (7)	25565 (5)	21564 (4)	254 (3)	159 (2)	266 (3)	-46 (9)	25 (4)	107 (8)
Cl(1)	3031 (6)	4072 (4)	2251 (4)	51 (4)	24 (2)	63 (4)	-32 (5)	-33 (6)	25 (5)
Cl(2)	1627 (7)	2902 (4)	869 (4)	66 (4)	41 (3)	33 (3)	-16 (5)	9 (5)	27 (4)
P(1)	802 (5)	1416 (3)	2025 (3)	27 (2)	16 (2)	29 (2)	2 (4)	13 (4)	3 (4)
P(2)	3785 (5)	2201 (3)	3224 (3)	24 (2)	18 (2)	32 (2)	-5 (3)	5 (4)	5 (3)
C(1.1)	377 (17)	1237 (13)	2885 (13)	14 (8)	23 (8)	48 (12)	-2 (13)	1 (16)	-10 (16)
C(2.1)	-34 (20)	407 (14)	3160 (12)	32 (11)	27 (9)	28 (10)	-13 (16)	10 (17)	-13 (15)
C(3.1)	-483 (22)	370 (16)	3801 (12)	40 (12)	37 (10)	29 (10)	-32 (18)	32 (17)	6 (17)
C(4.1)	-547 (21)	1131 (16)	4264 (13)	31 (11)	40 (11)	35 (12)	-10 (18)	3 (18)	-5 (19)
C(5.1)	-155 (19)	1968 (14)	3968 (13)	22 (9)	24 (9)	41 (11)	2 (15)	8 (16)	12 (16)
C(6.1)	310 (17)	2019 (13)	3347 (10)	19 (8)	25 (8)	16 (8)	-3 (13)	-7 (13)	-15 (13)
C(7.1)	1184 (20)	292 (14)	1601 (11)	37 (11)	26 (9)	18 (9)	3 (16)	3 (16)	-15 (14)
C(8.1)	2150 (22)	-192 (15)	2245 (18)	25 (11)	25 (10)	88 (18)	15 (18)	3 (22)	15 (23)
C(9.1)	104 (22)	-380 (14)	1383 (14)	43 (12)	23 (9)	43 (13)	-28 (17)	15 (20)	-21 (17)
C(10.1)	1741 (22)	495 (15)	950 (15)	35 (12)	28 (10)	59 (14)	3 (17)	15 (21)	-41 (20)
C(11.1)	-762 (21)	1829 (15)	1456 (11)	40 (11)	34 (10)	16 (8)	10 (18)	-3 (15)	20 (15)
C(12.1)	-1822 (20)	1290 (17)	1680 (13)	25 (10)	53 (12)	31 (11)	12 (18)	9 (17)	8 (19)
C(13.1)	-919 (22)	1744 (15)	598 (12)	39 (11)	33 (10)	22 (9)	-0 (17)	4 (17)	-0 (16)
C(14.1)	-954 (22)	2854 (16)	1625 (14)	41 (11)	37 (10)	50 (13)	26 (17)	18 (20)	24 (18)
C(1.2)	3618 (19)	1122 (12)	3737 (10)	31 (10)	17 (7)	13 (8)	3 (14)	-20 (14)	10 (12)
C(2.2)	4332 (21)	335 (14)	3675 (13)	37 (11)	19 (9)	32 (10)	12 (16)	-17 (18)	3 (15)
C(3.2)	4129 (25)	-446 (15)	4127 (13)	60 (15)	26 (10)	35 (11)	8 (19)	-19 (21)	-1 (17)
C(4.2)	3312 (25)	-425 (16)	4565 (13)	58 (15)	42 (11)	19 (10)	-29 (21)	-11 (20)	29 (17)
C(5.2)	2614 (20)	354 (14)	4621 (13)	28 (10)	29 (9)	38 (11)	-15 (16)	-4 (18)	-5 (17)
C(6.2)	2805 (18)	1102 (13)	4219 (13)	18 (9)	17 (8)	49 (12)	-10 (13)	-0 (16)	-1 (15)
C(7.2)	4136 (23)	3078 (14)	4019 (14)	44 (13)	23 (9)	45 (12)	-22 (18)	-2 (20)	8 (17)
C(8.2)	4728 (23)	2623 (19)	4779 (14)	48 (12)	46 (12)	45 (12)	-20 (24)	4 (19)	-1 (23)
C(9.2)	2900 (23)	3511 (16)	4135 (15)	47 (13)	26 (10)	57 (14)	18 (19)	25 (22)	-23 (20)
C(10.2)	5007 (24)	3869 (17)	3870 (18)	35 (13)	36 (12)	82 (19)	-27 (20)	-1 (25)	-27 (24)
C(11.2)	5185 (20)	2025 (16)	2799 (12)	27 (10)	46 (11)	31 (10)	-22 (17)	9 (17)	30 (18)
C(12.2)	4931 (20)	1259 (16)	2201 (14)	23 (10)	39 (11)	46 (12)	-4 (17)	27 (18)	13 (19)
C(13.2)	5464 (22)	2871 (18)	2362 (14)	32 (11)	60 (13)	40 (12)	-12 (19)	13 (19)	26 (20)
C(14.2)	6328 (23)	1825 (19)	3444 (15)	32 (12)	65 (15)	41 (13)	7 (21)	8 (20)	27 (22)

^a Thermal function is $T = \exp[-1/4(U_{11}h^2a^{*2} + U_{22}k^2b^{*2} + U_{33}l^2c^{*2} + U_{12}hka^*b^* + U_{13}hla^*c^* + U_{23}klb^*c^*)]$.

Table III. Selected Interatomic Distances (Å), Angles (Deg), and Torsion Angles (Deg) in the Molecule, with Esd's in Parentheses^a

Pt-Cl(1)	2.367 (6)	P(1)-C(1.1)	1.75 (3)
Pt-Cl(2)	2.349 (6)	P(1)-C(7.1)	1.90 (2)
Pt-P(1)	2.321 (5)	P(1)-C(11.1)	1.93 (2)
Pt-P(2)	2.344 (5)	P(2)-C(1.2)	1.86 (2)
C-C _{av} (phenyl)	1.40 (3)	P(2)-C(7.2)	1.91 (2)
C-C _{av} (<i>tert</i> -butyl)	1.55 (3)	P(2)-C(11.2)	1.91 (3)
P(1)-Pt-P(2)	107.3 (4)	Cl(1)-Pt-Cl(2)	84.2 (3)
P(1)-Pt-Cl(1)	156.5 (8)	P(2)-Pt-Cl(2)	152.1 (7)
P(1)-Pt-Cl(2)	89.6 (5)	P(2)-Pt-Cl(1)	87.9 (4)
C-C-C _{av} (phenyl)	120 (3)	C-C-C _{av} (<i>tert</i> -butyl)	108 (3)
Pt-P(1)-C(1.1)-C(2.1) ^b	37		
Pt-P(1)-C(1.1)-C(6.1)	75		
Pt-P(1)-C(7.1)-C(8.1)	-169		
Pt-P(1)-C(7.1)-C(9.1)	-43		
Pt-P(1)-C(7.1)-C(10.1)	-153		
Pt-P(1)-C(11.1)-C(12.1)	85		
Pt-P(1)-C(11.1)-C(13.1)	-35		
Pt-P(1)-C(11.1)-C(14.1)	104		
Pt-P(2)-C(1.2)-C(2.2)	-78		
Pt-P(2)-C(1.2)-C(6.2)	157		
Pt-P(2)-C(7.2)-C(8.2)	41		
Pt-P(2)-C(7.2)-C(9.2)	-81		
Pt-P(2)-C(7.2)-C(10.2)	-58		
Pt-P(2)-C(11.2)-C(12.2)	57		
Pt-P(2)-C(11.2)-C(13.2)	177		
Pt-P(2)-C(11.2)-C(14.2)			

^a The torsion angle A-B-C-D is counted positive when, looking around the B-C bond, the far bond is rotated clockwise with the respect to the near bond. ^b $\sigma_{av} = 4$.

Phosphine Conformations and Phosphine-Phosphine Interactions.

The *cis*-PtCl₂(P(*t*-Bu)₂Ph)₂ molecule is devoid of molecular symmetry due to the different conformations of the two phosphines. In both cases the P-C(Ph) distance is less than the P-C(*t*-Bu) separation by 0.09 Å [mean values 1.82 (3) and 1.91 (2) Å]. This feature has been

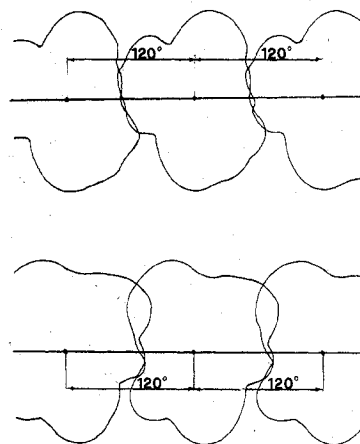


Figure 3. Top: representation according to the scheme of Figure 2 of Pt(P(*c*-Hx)₃)₃ complex. The three cones are equally oriented owing to the C₃ molecular symmetry. Bottom: one of the more acceptable orientations for the hypothetical Pt(P(*t*-Bu)₂Ph)₃ complex, obtained by considering the conformation displayed by P(1) phosphine in the present case and a C₃ molecular symmetry. Note that considerable mutual penetration of cones takes place.

previously observed in other alkyl-aryl phosphines.¹¹⁻¹⁴

The conformation of the phosphine P(1) is similar to that found in Pt(P(*t*-Bu)₂Ph)₃¹³ and Pd(P(*t*-Bu)₂Ph)₂¹⁴ while the P(2) phosphine exhibits a different conformation (see Pt-P-C-C angles in Table III). The nonbonding interactions between the atoms belonging to distinct phosphines within a single molecule do not indicate strain in spite of the *cis* arrangement. In fact only three short C...C contacts, ranging

(13) Otsuka, S.; Yoshida, T.; Matsumoto, M.; Nokatsu, K. *J. Am. Chem. Soc.* **1976**, *98*, 5850.

(14) Immirzi, A.; Musco, A. *J. Chem. Soc., Chem. Commun.* **1974**, 400.

Table IV. Selected Best Planes through Groups of Atoms in the Molecule^a

	A	B	C	D	δ
plane 1 (Pt, Cl(1), Cl(2), P(1), P(2))[Pt (0.031), Cl(1) (0.500), Cl(2) (-0.511), P(1) (0.403), P(2) (-0.424)]	-0.6732	0.4664	0.5738	1.9710	0.413
plane 2 (C(1.1)-C(6.1))[P(1) (-0.188), C(1.1) (-0.004), C(2.1) (0.003), C(3.1) (-0.010), C(4.1) (0.018), C(5.1) (-0.021), C(6.1) (0.014)]	0.9230	-0.1795	0.3405	1.8133	0.013
plane 3 (C(1.2)-C(6.2))[P(2) (0.033), C(1.2) (-0.009), C(2.2) (-0.003), C(3.2) (0.009), C(4.2) (-0.003), C(5.2) (-0.009), C(6.2) (0.015)]	0.7124	0.3256	0.62163	7.0415	0.009

^a The equations are in the form $Ax + By + Cz = D$, where x, y , and z are orthogonal coordinates. δ is the mean square displacement (in Å). Deviations of the relevant atoms from the plane are given in square brackets.

Table V. List of the Shortest Packing Distances (in Å) Based on Atomic Radii (1.80 for Aromatic Carbons, 1.95 for Methyl Groups, 1.10 for Hydrogens, and 1.80 Å for Chlorines)^a

C(8.1)	C(13.2) ⁱⁱ	3.86
C(9.1)	C(9.2) ⁱ	3.67*
C(4.1)	C(14.2) ^{vi}	3.55*
C(3.2)	C(3.2) ^{iv}	3.59
C(3.2)	C(4.2) ^{iv}	3.55
H(3.1)	Cl(2) ⁱ	2.80
H(5.1)	C(13.1) ^v	2.74*
H(3.2)	C(13.2) ⁱⁱ	2.96
H(3.1)	H(5.2) ⁱⁱⁱ	2.11

^a The packing operators indicated are as follows: i = $-x, y - 1/2, 1/2 - z$; ii = $1 - x, y - 1/2, 1/2 - z$; iii = $-x, -y, 1 - z$; iv = $1 - x, -y, 1 - z$; v = $x, 1/2 - y, z - 1/2$; vi = $x - 1, y, z$.

from 3.20 to 3.26 Å, are present.

The *cis* structure of the present compound with the P-M-P angle of 107.3° seems to indicate a certain ability of the bulky P(*t*-Bu)₂Ph ligands to coordinate on a metal atom, meshing the protrusions of a molecule with the hollows of another and achieving a P-M-P angle smaller than Tolman's cone aperture. A variable-aperture cone model (see ref 2 and 15) appears to us a more effective model for describing the phosphine behavior.

In Figure 2 the shape of the two cones of the present case is depicted by means of a polar diagram as suggested by Smith.¹⁶ The two cones are oriented like the phosphines in the complex, and the centers are separated by 107.3°, i.e., the actual P-M-P angle. It is evident that the actual orientation of the cones allows a very moderate cone overlap and explains the stability of the *cis*-PtCl₂L₂ complex.

This kind of representation is also useful for understanding the stability of PtL₃ complexes. In order that a given ML₃ complex be stable, it is necessary that each of the three cones be drawn near adjacent cones with little or no mutual overlap. Figure 3 (top) shows this representation for the C₃ symmetrical Pt(P(*c*-Hx)₃)₃ complex¹⁷ (*c*-Hx = cyclohexyl). It is interesting to consider the possibility that the inability to synthesize Pt(P(*t*-Bu)₂Ph)₃³ corresponds to the difficulty of finding some cone orientation with acceptable overlap. Among the numerous trials, using both the ligand conformation observed in the present case and C₃ symmetry, one of the more acceptable solutions is shown in Figure 3 (bottom).

Conclusions

The steric behavior of tertiary phosphines in coordination complexes seems to be predictable on the basis of their variable-aperture cone models. The case of PtCl₂(P(*t*-Bu)₂Ph)₂ demonstrates the importance of considering the irregular cone as a whole with its protrusions and hollows. Tolman's cone angle θ and Immirzi and Musco's solid angles Ω are only overall measures which ought to be considered with caution. As a matter of fact, Ω values seem to be more meaningful than θ ones in most cases (see ref 2). In the current case, for instance, while θ values are much greater than $1/3(360^\circ)$ for both the phosphines (170° in both cases), the Ω angle can achieve values $< 1/3(4\pi)$ for P(*c*-Hx)₃ (4.18 rad in Pt(P(*c*-Hx)₃)₃¹⁷), whereas it is never less than 4.51 rad for P(*t*-Bu)₂Ph (observed for P(2) phosphine in our case).

Registry No. *cis*-PtCl₂(P(*t*-Bu)₂Ph)₂, 73889-59-5.

Supplementary Material Available: A list of the observed and calculated structure factors (31 pages). Ordering information is given on any current masthead page.

(15) Alyea, E. C.; Dias, S. A.; Ferguson, G.; Restivo, R. J. *Inorg. Chem.* **1977**, *16*, 232.

(16) Smith, J. D.; Oliver, J. D. *Inorg. Chem.* **1978**, *17*, 2585.

(17) Immirzi, A.; Musco, A.; Mann, B. E. *Inorg. Chim. Acta* **1977**, *21*, L37

Contribution from the Department of Chemistry,
The University of Texas at Austin, Austin, Texas 78712

Chloro[*cis*-2,10-diphenyl-2,10-diphospha- κ^2 P-6-thia- κ S-bicyclo[9.4.0]pentadeca-11(1),12,14-triene]copper. Synthesis and Structure¹

RAYMOND E. DAVIS,* EVAN P. KYBA,* A. MEREDITH JOHN, and JUDY M. YEP

Received January 16, 1980

The title complex was synthesized by reaction of the tridentate 11-membered macrocycle *cis*-2,10-diphenyl-2,10-diphospha-6-thiabicyclo[9.4.0]pentadeca-11(1),12,14-triene and either CuCl₂ under reducing conditions or CuCl. Spectroscopic (IR, ¹H, ³¹P, ¹³C NMR) properties are reported. Crystal structure data: $a = 15.746(2)$ Å, $b = 9.288(1)$ Å, $c = 18.476(2)$ Å, $\beta = 123.43(1)^\circ$, $R = 0.038$, $R_w = 0.054$, 3874 reflections with $I > 3.0\sigma_f$. X-ray data were collected at -35°C on a Syntex P2₁ autodiffractometer with monochromated Mo K α radiation. Triligation of the macrocycle to CuCl results in a tetrahedral complex in which the Cu-P (2.236(1), 2.248(1) Å) and Cu-Cl (2.249(1) Å) are shorter and the Cu-S bond (2.378(1) Å) is longer than usually observed in comparable Cu(I) complexes.

Tertiary phosphine complexes of Cu(I) have received considerable attention recently and are rich in stoichiometrical

variety of the type (R₃P)_{*n*}Cu_{*m*}X_{*m*} ($n = 1-4$; $m = 1, 2$; X = halogen).² Of particular interest to us have been the mo-